UTPT-94-35
hep-ph/9411412
November 1994

Momentum dependent quark mass in two-point correlators

B. Holdom and Randy Lewis
Department of Physics
University of Toronto
Toronto, Ontario
CANADA M5S 1A7

ABSTRACT

A momentum dependent quark mass may be incorporated into a quark model in a manner consistent with dynamically broken chiral symmetry. We use this to study the high Q^2 behavior of the vector, axialvector, scalar and pseudoscalar two-point correlation functions. Expanding the results to order $1/Q^6$, we show the correspondence between the dynamical quark mass and the vacuum condensates which appear in the operator product expansion of QCD. We recover the correct leading logarithmic Q^2 dependence of the various terms in the OPE, but we also find substantial subleading corrections which are numerically huge in a specific case. We conclude by using the vector minus axialvector correlator to estimate the $\pi^+ - \pi^0$ electromagnetic mass difference.

Introduction

For large momenta, the QCD running coupling is small and calculations may be carried out systematically by a perturbative expansion in the coupling. As the momentum scale is lowered, nonperturbative effects become significant and the coupling expansion is no longer useful. Consider specifically the physics of light quark flavors in the context of a two-point correlation function, $\Pi(q^2)$, which we define to be dimensionless. From a purely phenomenological standpoint, the onset of nonperturbative effects can be parameterized by a series of correction terms.[1]

$$\tilde{\Pi}(q^2) = \Pi(q^2) - \Pi_{pert}(q^2) = \sum_{n=1}^{N} \frac{C_n}{Q^{2n}} \tag{1}$$

Throughout this work, the tilde is used as a reminder that perturbative physics has been excluded. $Q^2 = -q^2$ is the (Euclidean) momentum squared and the C_n depend at most logarithmically on Q^2. When Q^2 (which we always choose to be positive) is not too small, this series is dominated by the first few terms and can be used to perform calculations at lower Q^2 than is possible using only the perturbative coupling expansion. (1) is actually an operator product expansion (OPE) and the C_n are known functions of various nonzero vacuum condensates.[1]

The chiral symmetry breaking vacuum condensate with the lowest mass dimension is $\langle \overline{q}q \rangle$, and it (when multiplied by a current quark mass) will contribute to C_2 in (1). There is one other condensate in C_2, $\left\langle \alpha_s G^r_{\mu\nu} G^{r\,\mu\nu} \right\rangle$, but it does not break chiral symmetry and will not be of direct interest in what follows. Since there are no condensates with mass dimension two, C_1=0 in QCD.

The existence of a nonzero $\langle \overline{q}q \rangle$ implies an effective quark mass[2], and this in turn modifies the QCD Ward-Takahashi (WT) identities for the couplings of vector and axialvector fields to quarks. The complete two-point correlator in QCD is shown in Fig. 1, where one vertex is a bare $\gamma_\mu[\gamma_5]$ but the other vertex and both quark propagators represent fully-dressed nonperturbative quantities that must satisfy the WT identities. In what follows we will consider only the contributions of the effective quark mass to these nonperturbative quantities, and it will be shown that for both the vector and axialvector correlators, a "minimal" WT vertex correctly reproduces C_1 and the $\langle \overline{q}q \rangle$ term of C_2. We obtain expressions for C_3 in the vector and axialvector cases which have the known

leading logarithmic running, and we point out the possibility of substantial corrections in C_3 due to terms that are formally suppressed by logarithms.

The same diagram (Fig. 1) also represents the scalar and pseudoscalar two-point correlators in QCD, although there are no WT identities to constrain the corresponding vertices. If the full scalar or pseudoscalar vertex is approximated by a bare one, C_2 is not generated in its correct form. Improved scalar and pseudoscalar vertices can be found by appealing to the gauged nonlocal constituent (GNC) quark model.[3]

The GNC Lagrangian contains constituent quarks with momentum dependent masses and pseudoscalar mesons, constructed to model dynamically broken chiral symmetry. The couplings of vector and axialvector fields to quarks are precisely the "minimal" WT vertices mentioned above. Although the GNC Lagrangian originally included the scalar and pseudoscalar fields in a trivial way[3], the Lagrangian allows for a natural extension of these couplings in a manner analogous to its vector and axialvector couplings. For the case of the scalar correlator we verify that this produces the correct expressions for the chiral symmetry breaking pieces of C_2. C_3 also has the correct leading logarithmic running, but here we find enormous subleading correction terms as well.

It is important to stress that we will use the GNC model only to determine the form of the nonperturbative propagators and vertices appearing in the general correlator of QCD in Fig. 1. Our main goal is to study the relation between the $1/Q^2$ expansion of these correlators and the momentum dependent mass function. We will need to consider the low energy behavior of these correlators only when we treat the pion mass difference. At low energies we may apply the GNC model directly, since it has been shown to model low energy phenomenology rather well[3][4]. Thus at low energy the correlators will be described by the GNC model diagrams of Fig. 2, and at high energies they will be described by Fig. 1. The GNC model includes the pseudo-Goldstone bosons of QCD, and virtual effects of these mesons are accounted for in the low energy contribution according to the standard chiral Lagrangian approach. Meson loops are naturally cutoff in the model at the point where these particles lose their particle-like nature.

The vector minus axialvector two-point correlator is of special interest in our study since it would vanish if chiral symmetry was not broken. We will choose an explicit form for the effective quark mass which becomes the known form[2] at large momentum scales and which resembles the successful[3][4] GNC ansatz at small scales. We can then calculate the vector minus axialvector correlator numerically at any momentum scale by

matching the low energy GNC model (Fig. 2 plus meson loops) to our high energy model (Fig. 1) at an intermediate scale. An integral over all momenta produces the $\pi^+ - \pi^0$ electromagnetic mass difference[5].

The general $1/Q^2$ expansion

It is convenient to express the vector, axialvector, scalar and pseudoscalar two-point correlators in terms of dimensionless functions of Q^2,

$$i\int d^4x\ e^{iq\cdot x}\left\langle 0|\mathrm{T}\{V_\mu^a(x)V_\nu^b(0)\}|0\right\rangle = (q_\mu q_\nu - q^2 g_{\mu\nu})^V\Pi^{ab}(Q^2) \quad (2)$$

$$i\int d^4x\ e^{iq\cdot x}\left\langle 0|\mathrm{T}\{A_\mu^a(x)A_\nu^b(0)\}|0\right\rangle = (q_\mu q_\nu - q^2 g_{\mu\nu})^{A,1}\Pi^{ab}(Q^2) - q_\mu q_\nu{}^{A,0}\Pi^{ab}(Q^2) \quad (3)$$

$$i\int d^4x\ e^{iq\cdot x}\left\langle 0|\mathrm{T}\{S^a(x)S^b(0)\}|0\right\rangle = Q^2\ {}^S\Pi^{ab}(Q^2) \quad (4)$$

$$i\int d^4x\ e^{iq\cdot x}\left\langle 0|\mathrm{T}\{P^a(x)P^b(0)\}|0\right\rangle = Q^2\ {}^P\Pi^{ab}(Q^2) \quad (5)$$

where a, b are SU(N_f) flavor indices. Throughout this work we will restrict the discussion to light quarks. According to Fig. 1 we must determine the full quark propagator and the full vertex for each correlator.

The most general quark propagator is

$$i\mathcal{S}(q) = \frac{iZ(Q^2)}{\not{q} - \Sigma(Q^2)} \quad (6)$$

If we think of writing the nonperturbative contributions to the inverse propagator as a $1/Q^2$ series, analogous to (1), there are only two condensates with mass dimension less than five: $\langle\overline{q}q\rangle$ and $\left\langle\alpha_s G^r_{\mu\nu}G^{r\,\mu\nu}\right\rangle$. In the limit of vanishing current quark masses, we see on purely dimensional grounds that $Z(Q^2)$ cannot contain $\langle\overline{q}q\rangle$ while $\Sigma(Q^2)/Z(Q^2)$ is independent of $\left\langle\alpha_s G^r_{\mu\nu}G^{r\,\mu\nu}\right\rangle$. For our analysis of chiral symmetry breaking, we will set $Z(Q^2)$=1 at the expense of omitting the gluon condensate (which contains no information about chiral symmetry breaking) as well as other effects at higher order in the $1/Q^2$ series. Recall that the $\pi^+ - \pi^0$ electromagnetic mass difference is independent of $\left\langle\alpha_s G^r_{\mu\nu}G^{r\,\mu\nu}\right\rangle$.

We will retain $\Sigma(Q^2)$ with the correct asymptotic behavior[2]

$$\Sigma(Q^2) \to \frac{-4\pi\alpha_s(Q)}{3Q^2}\langle\overline{q}q\rangle \quad , \text{ as } Q^2 \to \infty \quad (7)$$

$$\langle\overline{q}q\rangle \equiv \langle\overline{q}q\rangle_Q = \langle\overline{q}q\rangle_\mu \left(\frac{\alpha_s(Q)}{\alpha_s(\mu)}\right)^{-d} \tag{8}$$

$$\alpha_s(Q) \to d\pi \left(\ln\frac{Q^2}{\Lambda^2}\right)^{-1} \quad , \text{ as } Q^2 \to \infty \tag{9}$$

$d = 12/(33-2N_f)$ for N_f quark flavors, μ is a renormalization scale, Λ is the QCD scale and the current quark masses are set to zero. With this normalization, $\langle\overline{q}q\rangle$ represents a single quark flavor summed over three colors and summed over Dirac indices.

The vector and axialvector vertices ${}^{V,A}\Gamma^a_\mu(p,q)$ are constrained to satisfy the Ward-Takahashi identities.

$$q^\mu {}^V\Gamma^a_\mu(p,p+q) = \mathcal{S}^{-1}(p+q)\frac{\lambda^a}{2} - \frac{\lambda^a}{2}\mathcal{S}^{-1}(p) \tag{10}$$

$$q^\mu {}^A\Gamma^a_\mu(p,p+q) = \mathcal{S}^{-1}(p+q)\gamma_5\frac{\lambda^a}{2} + \gamma_5\frac{\lambda^a}{2}\mathcal{S}^{-1}(p) \tag{11}$$

The λ^a are flavor generators normalized by $\mathrm{Tr}(\lambda^a\lambda^b) = 2\delta^{ab}$. These identities, plus the requirement that the vertices contain no unphysical singularities, uniquely define the longitudinal part of the vector and axialvector vertices. We will choose the minimal vertices by ignoring any extra transverse pieces that may exist.[6] The resulting vertices, for incoming(outgoing) quark momentum $p(p' = p+q)$, are

$${}^V\Gamma^a_\mu(p,p') = \frac{\lambda^a}{2}\left[\gamma_\mu + (p+p')_\mu\left(\frac{\Sigma(P'^2)-\Sigma(P^2)}{P'^2-P^2}\right)\right] \tag{12}$$

$${}^A\Gamma^a_\mu(p,p') = \frac{\lambda^a}{2}\left[\gamma_\mu - \frac{q_\mu}{q^2}\left(\Sigma(P'^2)+\Sigma(P^2)\right)\right]\gamma_5 \tag{13}$$

Again, $P^2(P'^2) = -p^2(-p'^2)$. Notice that the vector vertex is completely free of singularities (assuming none are contained within $\Sigma(Q^2)$) but that the axialvector vertex is required to have a singular point. This massless state is the Goldstone boson of the dynamically broken symmetry — the pion for N_f=2.

There are no analogous identities to constrain the forms of the scalar and pseudoscalar vertices. One might be tempted to adopt the bare vertices

$${}^S\Gamma^a(p,p+q) = -\frac{\lambda^a}{2} \tag{14}$$

$${}^P\Gamma^a(p,p+q) = i\frac{\lambda^a}{2}\gamma_5 \tag{15}$$

but this will lead to a disagreement with the OPE. One must also decide how to include current quark mass effects. Our approach will be to appeal to the GNC quark model which is the minimal Lagrangian that contains constituent quarks with mass $\Sigma(Q^2)$ and which respects the dynamically broken chiral symmetry. The original GNC model[3] was used at low energy scales, and the external fields were coupled to quarks according to (12-15), but as stated above, the scalar and pseudoscalar couplings contradict the OPE at larger scales. We therefore propose the following "GNC$'$" model, which is identical to the original version except that the S and P fields now appear in the path-ordered exponential as well as in the local term. In Euclidean spacetime,

$$\begin{aligned}
\mathcal{L}_{\mathrm{GNC}'}(x,y) &= \overline{\psi}(x)\delta(x-y)\gamma^\mu[\partial_\mu - iV_\mu(y) - i\gamma_5 A_\mu(y) + \frac{1}{4}\gamma_\mu S(y) + \frac{i}{4}\gamma_\mu\gamma_5 P(y)]\psi(y) \\
&\quad +\overline{\psi}(x)\Sigma(x-y)\xi(x)X(x,y)\xi(y)\psi(y) \qquad (16)\\
X(x,y) &= \mathrm{P}\exp\left[-i\int_x^y \Gamma_\mu(z)dz^\mu\right] \qquad (17)\\
\Gamma_\mu(z) &= \frac{i}{2}\xi(z)[\partial_\mu - iV_\mu(z) - i\gamma_5 A_\mu(z) - \frac{1}{2}\gamma_\mu S(z) - \frac{i}{2}\gamma_\mu\gamma_5 P(z)]\xi^\dagger(z) + \\
&\quad \frac{i}{2}\xi^\dagger(z)[\partial_\mu - iV_\mu(z) + i\gamma_5 A_\mu(z) - \frac{1}{2}\gamma_\mu S(z) + \frac{i}{2}\gamma_\mu\gamma_5 P(z)]\xi(z) \qquad (18)\\
\xi(x) &= \exp\left[\frac{-i\gamma_5}{f}\sum_{a=1}^{8}\frac{\lambda^a}{2}\pi^a(x)\right] \qquad (19)
\end{aligned}$$

π^a contains the N_f^2-1 pseudoscalar mesons with decay constant f, and ψ is the N_f-plet of quark fields with mass $\Sigma(Q^2)$, the Fourier transform of $\Sigma(x-y)$. V_μ, A_μ, S, P are the external fields. $X(x,y)$ is a path-ordered exponential. Notice that we have assumed the same mass function $\Sigma(Q^2)$ for all quark flavors, which means that $\langle\overline{q}q\rangle$ is also flavor-independent.

The Feynman rules for the GNC$'$ model can be obtained from the Lagrangian (16) in a systematic manner as described in [7]. Notice that the meson pole which contributes to the full axialvector and pseudoscalar vertices now appears explicitly, as shown in Fig. 3. Although the GNC$'$ Lagrangian does not contain an explicit meson propagator, a propagator is generated by the quark loops of Fig. 4. The explicit calculation shows that the GNC$'$ Lagrangian does indeed reproduce the vector and axialvector vertices of (12-13). To include the effects of a nonzero current quark mass matrix, $\mathcal{M}$, we make the substitution

$$S(x) \to \mathcal{M} + S(x) \qquad (20)$$

For our purposes, we will only require terms linear in $\mathcal{M}$.

With Feynman rules in hand, the expressions for the two-point correlators of Fig. 1 are easily written down in the form of 4-momentum integrals. The integrands are largest when the momentum-squared flowing through one quark propagator is of order $\Sigma^2(0)$ so that the other propagator has a momentum-squared of order Q^2. When the results are expanded in powers of $\mathcal{M}$ and $1/Q^2$, we obtain a series of the form (1). The simple procedure of expanding the *integrand* in $1/Q^2$ generates integral expressions for the various C_n, and these integrals become more divergent for increasing n. We stress that the full expression for each $\tilde{\Pi}(Q^2)$ is finite and it is only the simple expansion technique which creates apparent divergences. Our results are

$$
\begin{aligned}
{}^{V}\tilde{\Pi}^{ab}(Q^2) &= \frac{\mathcal{M}^{ab}}{4Q^4}(-\Upsilon_1 + \ldots) - \frac{\delta^{ab}}{Q^6}\left(\Upsilon_1 Q^2 \Sigma(Q^2) + \frac{\Upsilon_2}{3} + \ldots\right) + \mathcal{O}\left(\frac{1}{Q^8}\right) && (21)\\
{}^{A,1}\tilde{\Pi}^{ab}(Q^2) &= \frac{\mathcal{M}^{ab}}{4Q^4}(\Upsilon_1 + \ldots) + \frac{\delta^{ab}}{Q^6}\left(\Upsilon_1 Q^2 \Sigma(Q^2) + \frac{\Upsilon_2}{6} + \ldots\right) + \mathcal{O}\left(\frac{1}{Q^8}\right) && (22)\\
{}^{A,0}\tilde{\Pi}^{ab}(Q^2) &= \frac{\mathcal{M}^{ab}}{2Q^4}(-\Upsilon_1 + \ldots) + \mathcal{O}\left(\frac{1}{Q^8}\right) && (23)\\
{}^{S}\tilde{\Pi}^{ab}(Q^2) &= \frac{\mathcal{M}^{ab}}{8Q^4}(-3\Upsilon_1 + \ldots) - \frac{\delta^{ab}}{Q^6}\left(\frac{3\Upsilon_1}{2} Q^2 \Sigma(Q^2) - \Upsilon_2 + \ldots\right) + \mathcal{O}\left(\frac{1}{Q^8}\right) && (24)\\
{}^{P}\tilde{\Pi}^{ab}(Q^2) &= \mathcal{O}\left(\frac{1}{Q^2}\right) && (25)
\end{aligned}
$$

We have defined

$$
\mathcal{M}^{ab} = \mathrm{Tr}\left(\mathcal{M}\left\{\lambda^a, \lambda^b\right\}\right) \tag{26}
$$

where $\left\{\lambda^a, \lambda^b\right\}$ is an anticommutator. The ellipses at a given order in $1/Q^2$ denote the undetermined contributions from divergent integrals which exist at higher order in the naive integrand expansion. (We will discuss the calculation of these terms below.) We have not shown the current mass matrix $\mathcal{M}$ except for the leading logarithmic terms at order $Q^{-4}(\ln Q^2)^d$, where we have retained the terms linear in $\mathcal{M}$. The Υ_n are one-dimensional integrals which diverge logarithmically and require renormalization. When (7) is used to evaluate these integrals from the QCD scale Λ up to a cutoff Q^2, we obtain

$$
\Upsilon_1 \equiv \frac{3}{4\pi^2}\int_{\Lambda^2}^{Q^2} dx \frac{x\Sigma(x)}{x + \Sigma^2(x)} = -\langle \overline{q} q \rangle \tag{27}
$$

$$\Upsilon_2 \equiv \frac{3}{4\pi^2}\int_{\Lambda^2}^{Q^2} dx \frac{x^2\Sigma^2(x)}{x+\Sigma^2(x)} = \frac{-4d^2}{3(1-2d)}\pi^2 \langle\overline{q}q\rangle^2 \left(\ln\frac{Q^2}{\Lambda^2}\right)^{-1} \tag{28}$$

To leading order in α_s, the OPE in QCD gives[1]

$$^{V}\tilde{\Pi}^{ab}(Q^2) = \frac{\mathcal{M}^{ab}}{4Q^4}\langle\overline{q}q\rangle + \frac{\delta^{ab}}{24\pi Q^4}\left\langle\alpha_s G^r_{\mu\nu}G^{r\,\mu\nu}\right\rangle - \frac{\mathcal{A}^{ab}(\gamma_\mu\gamma_5)}{2Q^6} - \frac{\mathcal{B}^{ab}}{18Q^6} + \mathcal{O}\left(\frac{1}{Q^8}\right) \tag{29}$$

$$^{A,1}\tilde{\Pi}^{ab}(Q^2) = \frac{-\mathcal{M}^{ab}}{4Q^4}\langle\overline{q}q\rangle + \frac{\delta^{ab}}{24\pi Q^4}\left\langle\alpha_s G^r_{\mu\nu}G^{r\,\mu\nu}\right\rangle - \frac{\mathcal{A}^{ab}(\gamma_\mu)}{2Q^6} - \frac{\mathcal{B}^{ab}}{18Q^6} + \mathcal{O}\left(\frac{1}{Q^8}\right) \tag{30}$$

$$^{A,0}\tilde{\Pi}^{ab}(Q^2) = \frac{-\mathcal{M}^{ab}}{2Q^4}\langle\overline{q}q\rangle + \mathcal{O}\left(\frac{1}{Q^8}\right) \tag{31}$$

$$^{S}\tilde{\Pi}^{ab}(Q^2) = \frac{3\mathcal{M}^{ab}}{8Q^4}\langle\overline{q}q\rangle + \frac{\delta^{ab}}{16\pi Q^4}\left\langle\alpha_s G^r_{\mu\nu}G^{r\,\mu\nu}\right\rangle + \frac{\sqrt{4\pi\alpha_s}}{16Q^6}\mathcal{M}^{ab}\langle\overline{q}\sigma_{\mu\nu}\tau^r qG^{r\,\mu\nu}\rangle + \frac{\mathcal{A}^{ab}(\sigma_{\mu\nu})}{4Q^6} + \frac{\mathcal{B}^{ab}}{12Q^6} + \mathcal{O}\left(\frac{1}{Q^8}\right) \tag{32}$$

$$^{P}\tilde{\Pi}^{ab}(Q^2) = \frac{-\mathcal{M}^{ab}}{8Q^4}\langle\overline{q}q\rangle + \frac{\delta^{ab}}{16\pi Q^4}\left\langle\alpha_s G^r_{\mu\nu}G^{r\,\mu\nu}\right\rangle + \frac{\mathcal{A}^{ab}(\sigma_{\mu\nu}\gamma_5)}{4Q^6} + \frac{\mathcal{B}^{ab}}{12Q^6} + \mathcal{O}\left(\frac{1}{Q^8}\right) \tag{33}$$

We have defined

$$\mathcal{A}^{ab}(\Gamma_{\mu\ldots}) = \pi\alpha_s\left\langle\overline{\psi}\Gamma_{\mu\ldots}\tau^r\lambda^a\psi\overline{\psi}\Gamma^{\mu\ldots}\tau^r\lambda^b\psi\right\rangle \tag{34}$$

$$\mathcal{B}^{ab} = \pi\alpha_s\left\langle\overline{\psi}\gamma_\mu\tau^r\left\{\lambda^a,\lambda^b\right\}\psi\sum_{q=u,d,s,\ldots}\overline{q}\gamma^\mu\lambda^r q\right\rangle \tag{35}$$

Recall that q denotes a single quark flavor whereas ψ is the quark N_f-plet. The τ^r are SU(3) color generators normalized by $\mathrm{Tr}(\tau^r\tau^s) = 2\delta^{rs}$.

A comparison of (21-25) and (29-33) gives our expressions for the leading vacuum condensates. At the outset of this section we neglected $\left\langle\alpha_s G^r_{\mu\nu}G^{r\,\mu\nu}\right\rangle$ contributions to the quark propagator, and we now see explicitly that $\left\langle\alpha_s G^r_{\mu\nu}G^{r\,\mu\nu}\right\rangle$ is absent from our results for the correlators. The results verify, for all correlators except possibly the pseudoscalar, that the model correctly generates no dimension two condensates. The integrand of the pseudoscalar expression could not be expanded in our simple manner beyond dimension two without introducing quadratically divergent integrals. Whether or not the offending terms actually sum to zero cannot be determined with this technique. At order $1/Q^4$, the terms in the vector, axialvector and scalar correlators which involve the current quark

masses also agree with the OPE if we can neglect the ellipses in (21-24). (We will justify the neglect of these terms below.) The successful result for the scalar correlator in particular is a reflection of the scalar vertex present in the GNC′ Lagrangian.

At dimension six, we neglect $\mathcal{M}$ corrections and find expressions for the 4-quark condensates that appear in each of three correlators.

$$\begin{aligned} 9\mathcal{A}^{ab}(\gamma_\mu) + \mathcal{B}^{ab} &= -18\Upsilon_1 Q^2 \Sigma(Q^2)\delta^{ab} - 3\Upsilon_2 \delta^{ab} + \ldots \\ &= -4d\left(6 - \frac{d}{(1-2d)}\right)\pi^2\delta^{ab}\left\langle\overline{q}q\right\rangle^2\left(\ln\frac{Q^2}{\Lambda^2}\right)^{-1} + \ldots \qquad (36) \\ 9\mathcal{A}^{ab}(\gamma_\mu\gamma_5) + \mathcal{B}^{ab} &= 18\Upsilon_1 Q^2 \Sigma(Q^2)\delta^{ab} + 6\Upsilon_2 \delta^{ab} + \ldots \\ &= 4d\left(6 - \frac{2d}{(1-2d)}\right)\pi^2\delta^{ab}\left\langle\overline{q}q\right\rangle^2\left(\ln\frac{Q^2}{\Lambda^2}\right)^{-1} + \ldots \qquad (37) \\ 3\mathcal{A}^{ab}(\sigma_{\mu\nu}) + \mathcal{B}^{ab} &= -18\Upsilon_1 Q^2 \Sigma(Q^2)\delta^{ab} + 12\Upsilon_2 \delta^{ab} + \ldots \\ &= -4d\left(6 + \frac{4d}{(1-2d)}\right)\pi^2\delta^{ab}\left\langle\overline{q}q\right\rangle^2\left(\ln\frac{Q^2}{\Lambda^2}\right)^{-1} + \ldots \qquad (38) \end{aligned}$$

Recollection of the Q^2 dependence of $\langle\overline{q}q\rangle$ given in (8) reveals that these functions exhibit the known $(\ln Q^2)^{2d-1}$ dependence on Q^2.[1] However, the presence of undetermined contributions at the same order in $1/Q^2$ prevents us from using this approach to obtain complete expressions for these condensates. To proceed, we examine a specific example in detail.

Rigorous $1/Q^2$ expansion for a specific mass function

The loop integrations from Fig. 1 can be performed rigorously for the simple mass function which has typically been used in low energy GNC calculations.

$$\Sigma(Q^2) = \frac{(A+1)m_0^3}{Am_0^2 + Q^2} \qquad (39)$$

$m_0 \sim 300$MeV represents the scale of the constituent quark mass and the data require $2 \lesssim A \lesssim 3$.[3] Our goal is to build a mass function which becomes (39)[(7)] in the limit of small[large] Q^2, but we begin with a discussion of (39) alone.

For any $A > 1.44$, the Euclidean propagator can be expanded in a convergent geometric series.

$$\frac{1}{Q^2 + \Sigma^2(Q^2)} = \frac{1}{Q^2 + Am_0^2} \sum_{k=0}^{\infty} \left(\frac{Am_0^2 - \Sigma^2(Q^2)}{Q^2 + Am_0^2} \right)^k \tag{40}$$

$$= \sum_{k=0}^{\infty} \sum_{l=0}^{k} \frac{k!}{l!(k-l)!} \frac{(Am_0^2)^{k-l}(-(A+1)^2 m_0^6)^l}{(Q^2 + Am_0^2)^{k+2l+1}} \tag{41}$$

When this relation is used for each propagator in the expression for a two-point correlator, the result contains four summations, but each term in the infinite series is an integral that can be evaluated by introducing a Feynman parameter in the standard fashion. The final expression does not, in general, resum to a simple functional form, but can be reduced to a single summation over hypergeometric functions which can then be summed numerically to any desired accuracy.

For example, the leading nonperturbative behavior of the vector correlator is

$${}^V\tilde{\Pi}^{ab}(Q^2) = \frac{-12}{(4\pi)^2} \mathcal{M}^{ab} t u^2 \left[\ln\left(\frac{1}{u}\right) - Y_V(v) \right] + \mathcal{O}(u^3) \tag{42}$$

where $Y_V(v)$ denotes the infinite series and

$$t \equiv \frac{A+1}{A^2 m_0} \to \frac{\Sigma^2(0)}{Q^2 \Sigma(Q^2)} \quad \text{as } Q^2 \to \infty \tag{43}$$

$$u \equiv \frac{Am_0^2}{Q^2} \to \frac{\Sigma(Q^2)}{\Sigma(0)} \quad \text{as } Q^2 \to \infty \tag{44}$$

$$v \equiv \frac{(A+1)^2}{A^3} \to \frac{\Sigma^3(0)}{Q^2 \Sigma(Q^2)} \quad \text{as } Q^2 \to \infty \tag{45}$$

For any $A > 1.44$, $Y_V(v)$ is well-approximated by the following simple form.

$$Y_V(v) \approx \frac{1}{2} - 0.45 v^{0.44} \tag{46}$$

The value of $Y_V(0)$ is exact, and all derivatives at v=0 are infinite in the true (series) expression as well as in this approximation.

If we assume (incorrectly) that this result remains valid when (39) is modified to be consistent with the correct asymptotic form of (7), then we get

$${}^V\tilde{\Pi}^{ab}(Q^2) = \frac{d}{4Q^4} \mathcal{M}^{ab} \langle \overline{q} q \rangle \left(\ln \frac{Q^2}{\Lambda^2} \right)^{-1} \left[\ln\left(\frac{\tilde{v} Q^2}{\Sigma^2(0)} \right) - Y_V(\tilde{v}) \right] + \mathcal{O}(u^3) \tag{47}$$

$$\tilde{v} \equiv \frac{\Sigma^3(0)}{Q^2 \Sigma(Q^2)} = \frac{-3\Sigma^3(0)}{4d\pi^2 \langle \overline{q} q \rangle} \left(\ln \frac{Q^2}{\Lambda^2} \right) \tag{48}$$

A comparison with (29) shows that we have obtained the correct leading logarithm except for a missing factor of $1/d$. This is to be expected. If we had put the true form of the mass function (7) into the integral of Fig. 1, there would have been an extra factor of $1/d$ which arises from the integration. This is easily demonstrated by computing the large Q^2 behavior of Υ_1, as defined in (27), with a cutoff.

$$\int_{\Lambda^2}^{Q^2} dx \frac{x\Sigma(x)}{x} \sim \int_{\Lambda^2}^{Q^2} dx \frac{1}{x} \left(\ln\frac{x}{\Lambda^2}\right)^{d-1} \sim \frac{1}{d}\left(\ln\frac{Q^2}{\Lambda^2}\right)^d \tag{49}$$

It is now clear that we were justified in neglecting the uncomputed terms containing $\mathcal{M}$ in (21-24) as was postulated in the previous section — the uncomputed terms produce functions $Y_V(v)$, $Y_A(v)$ and $Y_S(v)$ which are logarithmically suppressed relative to the computed term.

We now set $\mathcal{M}$=0 and consider the leading nonperturbative contributions to the vector, axialvector and scalar correlators. The pseudoscalar correlator could also be obtained, but the presence of the pion propagator (Figs. 3 and 4) makes the calculation rather tedious. The pion contribution to the axialvector correlator is slightly more pleasant, and the transverse nature of this correlator provides a valuable check on the calculation. The relation between the vector minus axialvector correlator and the pion mass difference, which we discuss below, is another incentive for pursuing the axialvector calculation. Our results are

$$^V\tilde{\Pi}^{ab}(Q^2) = \frac{34\delta^{ab}}{(4\pi)^2} u^3 v \left[\ln\left(\frac{1}{u}\right) - Z_V(v)\right] + \mathcal{O}(u^4) \tag{50}$$

$$^{A,1}\tilde{\Pi}^{ab}(Q^2) = \frac{-14\delta^{ab}}{(4\pi)^2} u^3 v \left[\ln\left(\frac{1}{u}\right) - Z_A(v)\right] + \mathcal{O}(u^4) \tag{51}$$

$$^S\tilde{\Pi}^{ab}(Q^2) = \frac{-15\delta^{ab}}{(4\pi)^2} u^3 v \left[\ln\left(\frac{1}{u}\right) - Z_S(v)\right] + \mathcal{O}(u^4) \tag{52}$$

where $Z_X(v)$ denote the infinite series and u, v are defined in (44-45). For any $A > 1.44$, the $Z_X(v)$ are well-approximated by the following simple forms.

$$Z_V(v) \approx \frac{67}{51} + 0.24\sqrt{v} \tag{53}$$

$$Z_A(v) \approx \frac{1}{42} + 0.40\sqrt{v} \tag{54}$$

$$Z_S(v) \approx \frac{67}{5} + \frac{1.20}{\sqrt{v}}\ln(1+v) \tag{55}$$

The values of $Z_X(0)$ are exact, and all derivatives at v=0 are infinite in the true (series) expressions as well as in these approximations.

If we consider a modification of (39) to make it consistent with the correct asymptotic form of (7), then we see that each correlator regains the known leading logarithmic behavior of (36-38). Moreover, we can now estimate the size of these condensates.

$$9\mathcal{A}^{ab}(\gamma_\mu) + \mathcal{B}^{ab} = 28d^2\pi^2\delta^{ab}\left\langle\overline{q}q\right\rangle^2\left(\ln\frac{Q^2}{\Lambda^2}\right)^{-2}\left[\ln\left(\frac{\tilde{v}Q^2}{\Sigma^2(0)}\right) - Z_A(\tilde{v})\right] \quad (56)$$

$$9\mathcal{A}^{ab}(\gamma_\mu\gamma_5) + \mathcal{B}^{ab} = -68d^2\pi^2\delta^{ab}\left\langle\overline{q}q\right\rangle^2\left(\ln\frac{Q^2}{\Lambda^2}\right)^{-2}\left[\ln\left(\frac{\tilde{v}Q^2}{\Sigma^2(0)}\right) - Z_V(\tilde{v})\right] \quad (57)$$

$$3\mathcal{A}^{ab}(\sigma_{\mu\nu}) + \mathcal{B}^{ab} = -20d^2\pi^2\delta^{ab}\left\langle\overline{q}q\right\rangle^2\left(\ln\frac{Q^2}{\Lambda^2}\right)^{-2}\left[\ln\left(\frac{\tilde{v}Q^2}{\Sigma^2(0)}\right) - Z_S(\tilde{v})\right] \quad (58)$$

We may compare these to those in the vacuum saturation approximation:

$$9\mathcal{A}^{ab}(\gamma_\mu) + \mathcal{B}^{ab} = \frac{224}{9}d\pi^2\delta^{ab}\left\langle\overline{q}q\right\rangle^2\left(\ln\frac{Q^2}{\Lambda^2}\right)^{-1} \quad (59)$$

$$9\mathcal{A}^{ab}(\gamma_\mu\gamma_5) + \mathcal{B}^{ab} = \frac{-352}{9}d\pi^2\delta^{ab}\left\langle\overline{q}q\right\rangle^2\left(\ln\frac{Q^2}{\Lambda^2}\right)^{-1} \quad (60)$$

$$3\mathcal{A}^{ab}(\sigma_{\mu\nu}) + \mathcal{B}^{ab} = \frac{-352}{9}d\pi^2\delta^{ab}\left\langle\overline{q}q\right\rangle^2\left(\ln\frac{Q^2}{\Lambda^2}\right)^{-1} \quad (61)$$

The two expressions have the same leading logarithmic dependence on Q^2, but the numerical factors in front differ. We could make similar remarks here as made in the discussion surrounding (47-49).

Of greater interest are the terms which are subleading to the leading logarithm, and which correspond to terms which are often neglected in approximations to QCD such as vacuum saturation. We may compare the terms in brackets in (47) and (56-58) to the leading logarithm, $\ln(Q^2/\Lambda^2)$. By making reasonable estimates of the various quantities involved,

$$100\text{MeV} \lesssim \Lambda \lesssim 300\text{MeV} \quad (62)$$

$$400\text{MeV} \lesssim \Sigma(0) \lesssim 500\text{MeV} \quad (63)$$

$$-(230\text{MeV})^3 \lesssim \left\langle\overline{q}q\right\rangle_\mu\left(\ln\tfrac{\mu^2}{\Lambda^2}\right)^{-d} \lesssim -(180\text{MeV})^3 \quad (64)$$

and by setting d=4/9 and Q=1GeV we obtain

$$2.4 \lesssim \quad \ln\left(\tfrac{Q^2}{\Lambda^2}\right) \quad \lesssim 4.6 \tag{65}$$

$$2.2 \lesssim \quad \ln\left(\tfrac{\tilde{v}Q^2}{\Sigma^2(0)}\right) - Y_V(\tilde{v}) \quad \lesssim 4.2 \tag{66}$$

$$1.7 \lesssim \quad \ln\left(\tfrac{\tilde{v}Q^2}{\Sigma^2(0)}\right) - Z_A(\tilde{v}) \quad \lesssim 2.3 \tag{67}$$

$$0.6 \lesssim \quad \ln\left(\tfrac{\tilde{v}Q^2}{\Sigma^2(0)}\right) - Z_V(\tilde{v}) \quad \lesssim 1.5 \tag{68}$$

$$-12.1 \lesssim \quad \ln\left(\tfrac{\tilde{v}Q^2}{\Sigma^2(0)}\right) - Z_S(\tilde{v}) \quad \lesssim -10.8 \tag{69}$$

The difference between the leading logarithm, $\ln(Q^2/\Lambda^2)$, and our actual result is small for the $1/Q^4$ term (vector correlator), but larger for the $1/Q^6$ terms in the various correlators. In the case of the scalar correlator the difference is remarkably enormous. The leading logarithm still controls the Q^2 dependence, but the magnitude of the implied condensates at a given value of Q^2 has been shifted substantially. We discuss the implications in the conclusion.

The $\pi^+ - \pi^0$ electromagnetic mass difference

Of most physical interest is the vector minus axialvector, or left-right (LR) correlator, which is a direct measure of chiral symmetry breaking. For $\mathcal{M}$=0,

$${}^{LR}\tilde{\Pi}(Q^2)\delta^{ab} = {}^{V}\tilde{\Pi}^{ab}(Q^2) - {}^{A}\tilde{\Pi}^{ab}(Q^2). \tag{70}$$

We now return to our full expression for the LR correlator, without a $1/Q^2$ expansion, and use it to calculate the $\pi^+ - \pi^0$ electromagnetic mass difference. This mass difference is given by[5]

$$\Delta m_\pi^2 = \frac{3\alpha}{4\pi f_\pi^2}\int_0^\infty dQ^2 \ \left[Q^2 \ {}^{LR}\tilde{\Pi}(Q^2)\right] \tag{71}$$

where α is the electromagnetic coupling. We will neglect the tiny effects of nonzero current quark masses. As discussed earlier, the large(small) Q^2 portion of the correlator will be obtained from Fig. 1(Fig. 2 plus meson loops). In fact, it will become evident as we proceed that we can get an upper bound on the mass difference by simply using Fig. 1 for all Q^2.

We must also decide how to extend the asymptotic form of $\Sigma(Q^2)$ given in (7) to smaller Q^2. The following simple ansatz contains four parameters: Am_0^2, Bm_0^3, C and

M^2. (As in [3], m_0 represents the scale of the constituent quark mass. Since it is not an independent parameter here, we are free to choose it to be numerically identical to its value in [3].)

$$\Sigma(Q^2) = \frac{Bm_0^3}{[Am_0^2 + Q^2]\left[1 + C\left\{\ln\left(1 + \frac{Q^2}{M^2}\right)\right\}^{1-d}\right]} \tag{72}$$

The motivation for this functional form comes from the $M \to \infty$ limit, where $\Sigma(Q^2)$ becomes the mass function used originally in the low energy GNC model. We wish to include the correct logarithmic behavior of the mass function at high energies without making significant changes to the original low energy form. The ten dimensionless quantities $L_i(\mu)$ which appear in the standard chiral Lagrangian[8] have been obtained from the GNC model (i.e. Fig. 2) in the $M \to \infty$ limit.[3][4] They are sensitive to the shape of the mass function, but not to the overall scale, so from this we can determine the value of Am_0^2.

$$(470 \text{ MeV})^2 \lesssim Am_0^2 \lesssim (550 \text{ MeV})^2 \tag{73}$$

One constraint on the three remaining parameters in (72) comes from demanding that $\Sigma(Q^2)$ satisfies the high energy behavior of (7), where the numerical value of $\langle\overline{q}q\rangle_\mu$ is known phenomenologically. This gives

$$\frac{Bm_0^3}{C} \approx \frac{-4d\pi^2}{3}\langle\overline{q}q\rangle_\mu \left(\ln\frac{\mu^2}{\Lambda^2}\right)^{-d} \tag{74}$$

Two more constraints arise from the low energy behavior of the LR correlator, which must reproduce the experimentally determined coefficients of the chiral Lagrangian. In the notation of [8], the relevant coefficients are F_0 and L_{10}.

$$Q^2\ {}^{LR}\tilde{\Pi}(Q^2) = F_0^2 + 4Q^2L_{10}(\mu) - \frac{N_fQ^2}{6(4\pi)^2}\left[\frac{5}{3} - \ln\left(\frac{Q^2}{\mu^2}\right)\right] + \mathcal{O}(Q^4) \tag{75}$$

N_f is the number of quark flavors. The dependence of L_{10} on the renormalization scale μ is canceled by the logarithm (which comes from internal meson loops), so that ${}^{LR}\tilde{\Pi}(Q^2)$ is independent of μ. We will eliminate the parameters Bm_0^3 and C by using the phenomenological values for $\langle\overline{q}q\rangle_\mu$ and F_0. The final parameter M will be determined by requiring the mass of (72) in the calculation of Fig. 2 to produce a value for L_{10} which is within, say, 25% of the original GNC result.

Before proceeding, we point out an interesting relation between the high and low energy calculations. From the evaluation of Fig. 2, we obtain

$$F_0^2 = \frac{3}{8\pi^2}\int_0^\infty ds \frac{s\Sigma(s)\left[2\Sigma(s) - s\Sigma'(s)\right]}{\left[s+\Sigma^2(s)\right]^2} \tag{76}$$

and a more lengthy expression for L_{10}. It turns out that exactly the same expression for F_0 happens to come from Fig. 1. The two expressions for L_{10} are not the same; Fig. 1 correctly predicts that L_{10} is negative, but the magnitude is only about half of the correct GNC result. This means that if Fig. 1 is used for all momenta, the slope of the LR correlator at Q^2=0 is too shallow (see Fig. 5), and an upper bound is obtained for Δm_π^2. We choose the strongest upper bound by using the smallest value of M which keeps L_{10} (of Fig. 2) within 25% of the original ($M \to \infty$) GNC result.

For definiteness, we use d=4/9 with the following inputs,

$$F_0 \approx 88\text{MeV} \tag{77}$$

$$\langle\overline{q}q\rangle_\mu \left(\ln\frac{\mu^2}{\Lambda^2}\right)^{-d} \approx -(220\text{MeV})^3 \tag{78}$$

Note that this last expression is independent of μ. With these values, the parameters B and C of (72) are of order unity, and the scale M is about 3 GeV. Fig. 1 then gives an upper bound on the electromagnetic pion mass difference.

$$m_{\pi^+} - m_{\pi^0}, \lesssim 5.1 \text{ MeV} \tag{79}$$

To obtain a direct estimate we will calculate the high energy expression for the LR correlator from Fig. 1 down to some intermediate scale Q^2_{high} and use Fig. 2 plus meson loops below the scale Q^2_{low} such that

$$Q^2\ {}^{LR}\tilde{\Pi}(Q^2_{low}) = Q^2\ {}^{LR}\tilde{\Pi}(Q^2_{high}) \equiv R^2 \tag{80}$$

Between Q^2_{low} and Q^2_{high}, this function will be approximated by the constant R^2. The LR correlator is plotted versus Q^2 in Fig. 5, and our result for the pion mass difference is shown in Fig. 6 as a function of R. The experimental value (after subtracting $m_d - m_u$ effects) is[8]

$$\left[m_{\pi^+} - m_{\pi^0}\right]_{expt} = 4.43 \pm 0.03 \text{ MeV} \tag{81}$$

and corresponds to 50MeV $\lesssim R \lesssim$ 55MeV. This implies that for this calculation, our low energy model is good up to a scale of order $Q^2_{low} \sim 400 - 450$MeV and our high energy model is good down to a scale of order $Q^2_{high} \sim 750 - 850$MeV. Both of these scales are very reasonable.

Conclusions

One consequence of the dynamical breakdown of chiral symmetry in QCD is the generation of a momentum dependent light quark mass. In the context of the vector, axialvector and scalar two-point correlators we have shown how this effective mass can be included systematically in calculations. The Ward-Takahashi identities and chiral symmetry are respected, as are the first few terms (at least) of the operator product expansion (OPE). An interesting result is the existence of terms at order $1/Q^6$ which do not contain the leading logarithm but which are not insignificant, especially in the case of the scalar correlator.

It appears that for the scalar two-point function a naive application of the OPE in conjunction with the vacuum saturation approximation does not adequately describe some expected physics of QCD, namely the physics associated with the dynamical quark mass. This is perhaps not surprising. Practitioners of sum rules have long claimed[9] that there is something deficient in the usual application of the OPE in the case of the scalar and pseudoscalar two-point functions. This is particularly clear in the pseudoscalar case, for which the conventional OPE does not adequately account for the pion appearing in the sum rule. This has led to speculations of additional contributions to these OPEs, including instantons[9], renormalons[10], and effective four-fermion interactions[11]. Our work indicates that the additional contributions will also have to reflect effects associated with chiral symmetry breaking, and in particular the momentum dependence of the dynamical quark mass. On the other hand in the case of the vector and axialvector two-point functions, the subleading terms in our analysis are not substantial enough to say that there is a serious conflict with standard treatments.

We have described in this work a minimal model. It could be extended for example by including an effective wavefunction renormalization parameter in the quark propagator, or by adding extra terms to the vertices which maintain the Ward-Takahashi identities and

the OPE. Interestingly enough, we find that the minimal model is sufficient to account for the $\pi^+ - \pi^0$ electromagnetic mass difference.

Acknowledgements

We thank Michael Luke for useful discussions. This research was supported in part by the Natural Sciences and Engineering Research Council of Canada.

References

[1] M.A. Shifman, A.I. Vainshtein and V.I. Zakharov, Nucl. Phys. **B147** (1979) 385.

[2] H.D. Politzer, Nucl. Phys. **B117** (1976) 397. See also K. Lane, Phys. Rev. **D10** (1974) 2605; H. Pagels, Phys. Rev. **D19** (1979) 3080.

[3] B. Holdom, Phys. Rev. **D45** (1992) 2534.

[4] B. Holdom, J. Terning, and K. Verbeek, Phys. Lett. **245B** (1990) 612 and **273B** (1991) 549E; B. Holdom, Phys. Lett. **292B** (1992) 150; B. Holdom, R. Lewis, and R.R. Mendel, Z. Phys. **C63** (1994) 71.

[5] T. Das, G. Guralnik, V. Mathur, F. Low and J. Young, Phys. Rev. Lett. **18** (1967) 759.

[6] J.S. Ball and T.-W. Chiu, Phys. Rev. **D22** (1980) 2542.

[7] J. Terning, Phys. Rev. **D44** (1991) 887.

[8] J. Gasser and H. Leutwyler, Nucl. Phys. **B250** (1985) 465.

[9] V.A. Novikov et. al., Nucl. Phys. **B191** (1981) 301, and references therein.

[10] V.I. Zakharov, Nucl. Phys. **B385** (1992) 452.

[11] K. Yamawaki and V.I. Zakharov, University of Michigan preprints UM-TH-94-19, hep-ph/9406373 and UM-TH-94-20, hep-ph/9406399.

Figure 1: The complete QCD contribution to a two-point correlator. Both propagators are full propagators; one vertex is full and the other vertex is a bare $\frac{\lambda^a}{2}[\gamma_5]$ or $\frac{\lambda^a}{2}\gamma_\mu[\gamma_5]$.

Figure 2: The quark contribution to a two-point correlator in the GNC$'$ model. Meson contributions are not shown.

Figure 3: The two distinct components of the full axialvector and pseudoscalar vertices as derived from the GNC$'$ model. The dashed line represents a pseudoscalar meson propagator which is generated from the diagrams of Fig. 4.

Figure 4: The GNC$'$ Lagrangian does not contain an explicit meson propagator, but a propagator is generated by the quark loop diagrams shown here.

Figure 5: The vector minus axialvector two-point correlator obtained from the GNC$'$ model at low energies and from Fig. 1 at high energies for a typical choice of parameters. The two pieces are matched to a constant, R^2, in the intermediate region.

Figure 6: The electromagnetic mass difference of the pion as a function of R, defined by (80), for a typical choice of parameters.

This figure "fig1-1.png" is available in "png" format from:

http://arXiv.org/ps/hep-ph/9411412v2

This figure "fig2-1.png" is available in "png" format from:

http://arXiv.org/ps/hep-ph/9411412v2

Figure 5

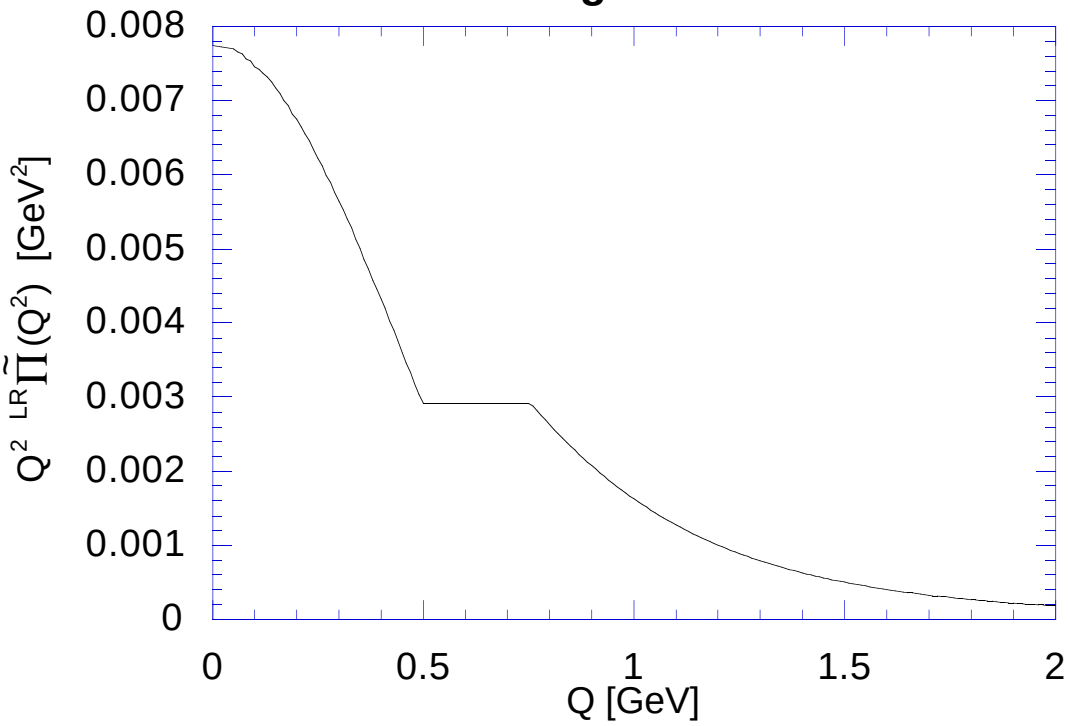

Figure 6

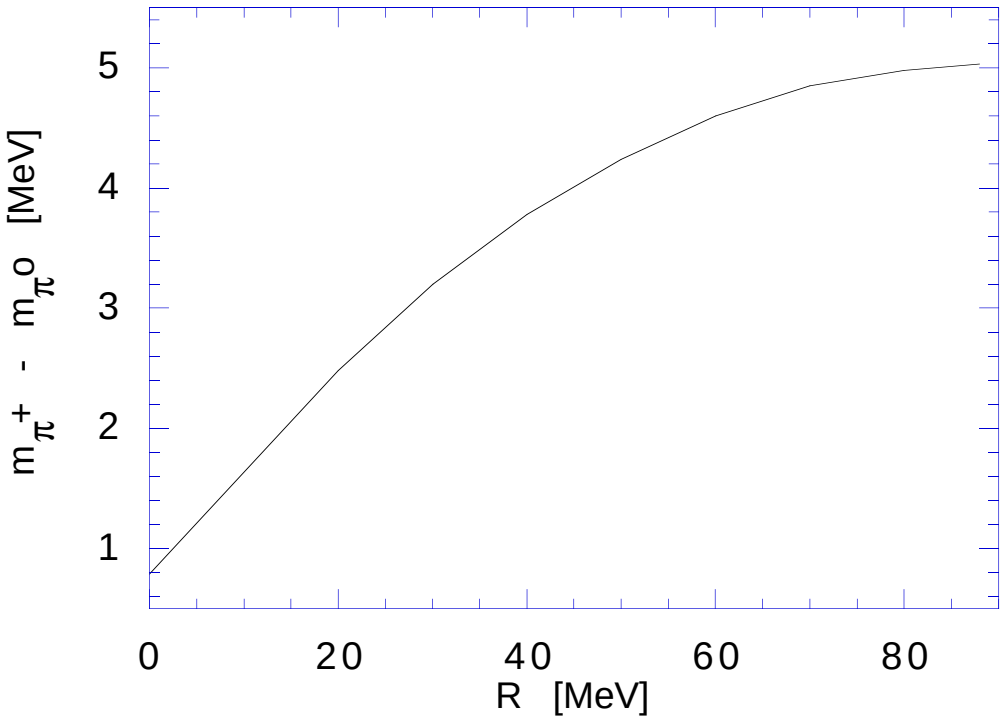

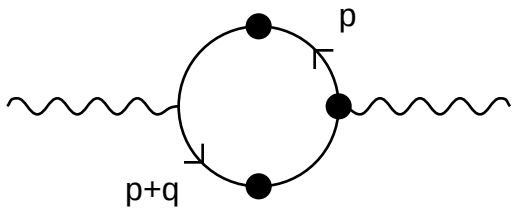

Figure 1

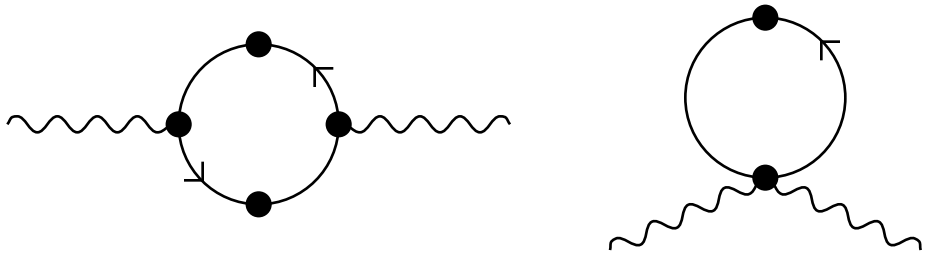

Figure 2

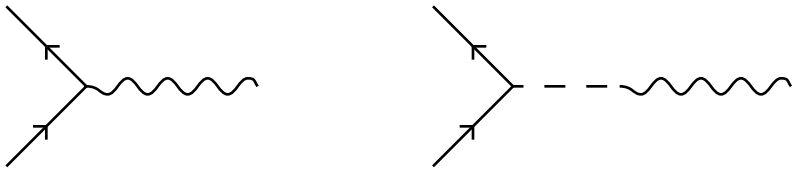

Figure 3

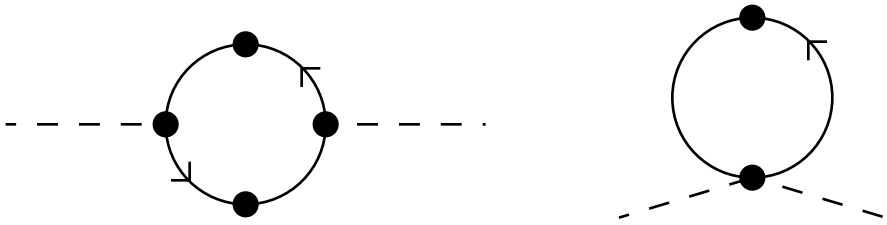

Figure 4